

Partial Gromov-Wasserstein Learning for Partial Graph Matching

Weijie Liu,¹ Chao Zhang,¹ Jiahao Xie,¹ Zebang Shen,² Hui Qian,¹ Nenggan Zheng¹

¹ Zhejiang University

² University of Pennsylvania

{westonhunter, qianhui, zczju, xiejh, zng}@zju.edu.cn, zebang@seas.upenn.edu

November 14, 2021

Abstract

Graph matching finds the correspondence of nodes across two graphs and is a basic task in graph-based machine learning. Numerous existing methods match every node in one graph to one node in the other graph whereas two graphs usually overlap partially in many real-world applications. In this paper, a partial Gromov-Wasserstein learning framework is proposed for partially matching two graphs, which fuses the partial Gromov-Wasserstein distance and the partial Wasserstein distance as the objective and updates the partial transport map and the node embedding in an alternating fashion. The proposed framework transports a fraction of the probability mass and matches node pairs with high relative similarities across the two graphs. Incorporating an embedding learning method, heterogeneous graphs can also be matched. Numerical experiments on both synthetic and real-world graphs demonstrate that our framework can improve the F1 score by at least 20% and often much more.

1 Introduction

Graph matching (alignment), aiming to determine the correspondence of nodes across different graphs, has a wide range of artificial intelligence applications, including graph classification [Schenker et al. \[2004\]](#); [Park et al. \[2010\]](#), entity alignment in knowledge graphs [Sun et al. \[2020\]](#); [Pei et al. \[2020\]](#), network retrieval [Berretti et al. \[2001\]](#); [Özer et al. \[2002\]](#), etc.

Graph matching involves finding a matching matrix $\mathbf{T} = [T_{ii'}]$ between two graphs \mathcal{G}^s and \mathcal{G}^t , where $T_{ii'} = 1$ if node i in \mathcal{G}^s maps to node i' in \mathcal{G}^t , and $T_{ii'} = 0$ otherwise. Assuming \mathcal{G}^s has fewer nodes than \mathcal{G}^t , generally, the matching matrix is identified by the solution to the following optimization formulation [Caetano et al. \[2009\]](#)

$$\min_{\mathbf{T} \in \mathcal{P}^f} \left[\sum_{ii'} k_{ii'} T_{ii'} + \sum_{ii'jj'} d_{ii'jj'} T_{ii'} T_{jj'} \right], \quad (1)$$

subject to the feasible domain

$$\mathcal{P}^f = \left\{ \mathbf{T} \mid \mathbf{T} \in [0, 1]^{m \times n}, \mathbf{T}\mathbf{1} = \mathbf{1}, \mathbf{T}^\top \mathbf{1} \leq \mathbf{1} \right\}, \quad (2)$$

where $k_{ii'}$ is the value of the cost function for the *unary assignment* $i \rightarrow i'$ and $d_{ii'jj'}$ is the cost for the *pairwise assignment* $(i, j) \rightarrow (i', j')$. Such formulation matches every node in \mathcal{G}^s to a node in \mathcal{G}^t and hence can be referred to as a *full matching* problem [Kazemi et al. \[2015\]](#).

The last several years have witnessed a flurry of research activities on the full matching problem. Some works determine the matching matrix by minimizing heuristic cost functions [Sun et al. \[2015\]](#); [Vijayan et al.](#)

[2015]; Mamano and Hayes [2017]. More recently, end-to-end deep learning frameworks for graph matching are proposed to simultaneously learn the assignment cost and the matching matrix Zanfir and Sminchisescu [2018]; Wang et al. [2019b,a], which however requires a large amount of ground truth node pairs to be available. Another line of works resolve the full matching problem from an *optimal transport* (OT) perspective, which models graphs as probability distributions and estimates the correspondence of nodes via calculating the *transport map* between two constructed distributions Maretic et al. [2019]; Xu et al. [2019b]; Titouan et al. [2019]; Maretic et al. [2020]; Barbe et al. [2020]. These OT-based methods exploit geometrical properties of the metric space and can estimate the node correspondence in an unsupervised/semi-supervised manner i.e. searching transport map with no/few ground truth node correspondences.

Despite the rapid progress of full matching methods, this setting is often inappropriate because the nodes of the two graphs may overlap partially in real-world applications. For example, a person that uses one social platform may not use the other. Wang et al. (2020b) reformulate the problem of partially matching as selecting reliable nodes in an *assignment graph* where each node is a candidate correspondence. Mainstream methods resolve this partial matching problem by replacing $\mathbf{T}\mathbf{1} = \mathbf{1}$ in the feasible domain (2) with $\mathbf{T}\mathbf{1} \leq \mathbf{1}$ Torresani et al. [2012]; Swoboda et al. [2019]; Sarlin et al. [2020]; Wang et al. [2020a]; Rolínek et al. [2020], i.e., solving (1) subject to the relaxed feasible domain

$$\mathcal{P}^p = \left\{ \mathbf{T} \mid \mathbf{T} \in [0, 1]^{m \times n}, \mathbf{T}\mathbf{1} \leq \mathbf{1}, \mathbf{T}^\top \mathbf{1} \leq \mathbf{1} \right\}. \quad (3)$$

Nevertheless, such relaxation limits the choice of cost functions and renders the matching matrix sensitive to $k_{ii'}$'s and $d_{ii'jj'}$'s, which can lead to degraded matching $\mathbf{T} = \mathbf{0}$ or still full matching with $\mathbf{T}\mathbf{1} = \mathbf{1}$ in extreme cases. Besides, this formulation does not consider the rank of the similarity values. To illustrate this, if $k_{ii'} > k_{jj'} > 0$ ¹, one always has $T_{ii'} = T_{jj'} = 0$ although pair (j, j') is comparatively more similar than (i, i') . We say (j, j') has a higher *relative similarity* value than (i, i') if $k_{ii'} > k_{jj'}$. Because $k_{ii'}$ is usually set as the negative inner product of embedding vectors of node i and i' Sarlin et al. [2020]; Rolínek et al. [2020] in deep learning-based matching methods, they may match few node pairs.

Another important problem is heterogeneous graph matching. Heterogeneous graphs often contain multi-typed nodes and structural relations (edges), encode richer information than its homogeneous counterparts, and are more prevalent Cai et al. [2018]; Zhang et al. [2019]; Zhu et al. [2014]; Wang et al. [2019c]. While most existing heterogeneous graph matching methods tackle graphs of specific scenarios Zheng et al. [2018]; Wang et al. [2019d]; Feng et al. [2019], Gu et al. (2018) propose heuristic methods for matching general heterogeneous graphs. However, the performance of these heuristic methods is sub-optimal and deteriorates rapidly as the noise level of the edges goes up Xu et al. [2019a]. Besides, existing methods only consider full matching. Partially matching general heterogeneous graphs therefore remains an open and challenging problem.

To bridge these gaps, we propose a novel partial graph matching framework based on partial OT Figalli [2010]; Caffarelli and McCann [2010]. We refer to the proposed framework as PPGM, which fuses the partial Gromov-Wasserstein distance and the partial Wasserstein distance as the objective and updates node embedding and transport map in an alternating manner. By transporting a fraction of the transport mass, our framework matches node pairs with high relative similarities across the two graphs. Under this framework, heterogeneous graphs can also be matched with an embedding learning method. Our contributions are summarized as follows.

- PPGM is the first partial Gromov-Wasserstein learning framework for partial graph matching. This framework models graphs as discrete distributions and resolves the partial matching problem via calculating the partial transport map that has minimum transportation cost. The partial transport map is calculated with a proximal point method, for which we prove convergence to a stationary point.
- Problem of partially matching heterogeneous graphs is explored. Utilizing a *random walk with restart* strategy, we take into account the type information of the vertices explicitly. A novel regularizer for embedding learning is further incorporated to increase the separability of inter-type embeddings and hence avoids aligning nodes of different types.

¹For simplicity, we assume $d_{ii'jj'} = 0$ for all (i, j) and (i', j') .

Experimental results demonstrate that the F1 score is improved by 20% and 77% on synthetic and real-world graphs respectively, which corroborate the efficacy of our framework. The rest of the paper is organized as follows. In Sec. 2, we introduce notation used in our paper and background of the proposed framework. We describe our framework in Sec. 3 and 4 for matching homogeneous graphs and heterogeneous graphs, respectively. Empirical results are given in Sec. 5.

2 Preliminaries

2.1 Notation

We use bold lowercase symbols, bold uppercase letters, uppercase calligraphic fonts, and Greek letters to denote vectors, matrices, spaces (sets), and measures, respectively. For example, $\alpha = \sum_i \delta(\mathbf{x}_i)$ where $\delta(\mathbf{x})$ is the Dirac at position \mathbf{x} , is a discrete measure supported on $\mathbf{x}_1, \dots, \mathbf{x}_n \in \mathcal{X}$. $\pi(\alpha, \beta)$ is a coupling measure between measures α and β , that is, for any subset $\mathcal{A} \subset \mathcal{X}$, $\pi(\mathcal{A} \times \mathcal{Y}) = \alpha(\mathcal{A})$, and for any $\mathcal{B} \subset \mathcal{Y}$, $\pi(\mathcal{X} \times \mathcal{B}) = \beta(\mathcal{B})$. $\Pi(\alpha, \beta)$ is the set of coupling measures. Σ^n is a probability symplecton with n bins, namely the set of probability vectors in \mathbb{R}_+^n . We denote the cardinality of set \mathcal{A} by $|\mathcal{A}|$. $(\cdot)^\top$ is the transpose of a vector. For two matrices \mathbf{A} and \mathbf{B} that are of the same size, $\langle \mathbf{A}, \mathbf{B} \rangle = \text{trace}(\mathbf{A}^\top \mathbf{B})$ is the Frobenius dot-product.

2.2 Optimal Transport

Let $\mathcal{X} = \{\mathbf{x}_i\}_{i=1}^m$ and $\mathcal{Y} = \{\mathbf{y}_j\}_{j=1}^n$ be two sample spaces. We assume two discrete probability distributions over \mathcal{X} and \mathcal{Y} respectively, i.e.,

$$\mathbf{p} = \sum_{i=1}^m p_i \delta(\mathbf{x}_i) \text{ and } \mathbf{q} = \sum_{j=1}^n q_j \delta(\mathbf{y}_j), \text{ s.t. } \mathbf{p} \in \Sigma^m, \mathbf{q} \in \Sigma^n.$$

Optimal transport (OT) addresses the problem of optimally transporting \mathbf{p} toward \mathbf{q} , given a cost K_{ij} measuring the distance between \mathbf{x}_i and \mathbf{y}_j . The p -Wasserstein distance between \mathbf{p} and \mathbf{q} is given by

$$W_p^p(\mathbf{p}, \mathbf{q}) = \min_{\mathbf{T} \in \Pi(\mathbf{p}, \mathbf{q})} \langle \mathbf{K}^p, \mathbf{T} \rangle,$$

where $\mathbf{K}^p = [K_{ij}^p]$ and $\mathbf{T} = [T_{ij}]$. Gromov-Wasserstein (GW) distance is a generalization of Wasserstein distance [Mémoli \[2011\]](#); [Patterson \[2019\]](#). Endowing the spaces \mathcal{X} and \mathcal{Y} with metrics (distance functions) $d_{\mathcal{X}}$ and $d_{\mathcal{Y}}$, the GW distance is defined as

$$GW_p^p(\mathbf{p}, \mathbf{q}) = \min_{\mathbf{T} \in \Pi(\mathbf{p}, \mathbf{q})} \sum_{i,j=1}^m \sum_{i',j'=1}^n D_{ii'jj'}^p T_{ii'} T_{jj'},$$

where $D_{ii'jj'} = |d_{\mathcal{X}}(\mathbf{x}_i, \mathbf{x}_{i'}) - d_{\mathcal{Y}}(\mathbf{y}_j, \mathbf{y}_{j'})|$.

The partial OT problem focuses on transporting only a fraction $0 \leq b \leq 1$ of the mass with minimum transportation costs [Figalli \[2010\]](#); [Caffarelli and McCann \[2010\]](#), that is, the set of admissible couplings is given by

$$\Pi^b(\mathbf{p}, \mathbf{q}) = \left\{ \mathbf{T} \mid \mathbf{T} \in \mathbb{R}_+^{m \times n}, \mathbf{T} \mathbf{1} \leq \mathbf{p}, \mathbf{T}^\top \mathbf{1} \leq \mathbf{q}, \mathbf{1}^\top \mathbf{T} \mathbf{1} = b \right\}.$$

and the partial Wasserstein distance and the partial GW distance are defined as follows

$$PW_p^p(\mathbf{p}, \mathbf{q}) = \min_{\mathbf{T} \in \Pi^b(\mathbf{p}, \mathbf{q})} \langle \mathbf{K}^p, \mathbf{T} \rangle,$$

$$PGW_p^p(\mathbf{p}, \mathbf{q}) = \min_{\mathbf{T} \in \Pi^b(\mathbf{p}, \mathbf{q})} \sum_{i,j=1}^m \sum_{i',j'=1}^n D_{ii'jj'}^p T_{ii'} T_{jj'}.$$

2.3 GW Distance for Graph Matching

Following Titouan et al. [2019]; Barbe et al. [2020], we consider undirected and attributed graphs as tuples of the form $\mathcal{G} = (\mathcal{V}, \mathcal{E}, \mathbf{X}, \mathbf{W}, f)$, where \mathcal{V} and \mathcal{E} are the sets of vertices² and edges of the graph, respectively. Node features are summarized in a $|\mathcal{V}| \times D$ matrix \mathbf{X} . $\mathbf{W} \in \mathbb{R}^{|\mathcal{V}| \times |\mathcal{V}|}$ assigns each observed edge $(u_i, u_j) \in \mathcal{E}$ for $u_i, u_j \in \mathcal{V}$ a weight w_{ij} . $f : \mathbf{X} \rightarrow \mathbf{Z}$ associates each vertex u_i with some representation vector \mathbf{z}_i . A cost matrix $\mathbf{C} = [c_{ij}] \in \mathbb{R}^{|\mathcal{V}| \times |\mathcal{V}|}$ is further defined with each c_{ij} characterizing the dissimilarity between vertices i and j .

Given two graphs, denoted as source graph \mathcal{G}^s and target graph \mathcal{G}^t , we assume that $|\mathcal{V}^s| \leq |\mathcal{V}^t|$, without loss of generality. Following the definition of *measure network* [Chowdhury and Mémoli, 2019; Xu et al., 2019b], we assign two distributions $\boldsymbol{\mu}^s = [\mu_i^s]$ and $\boldsymbol{\mu}^t = [\mu_i^t]$ to the two graphs, where

$$\mu_i^z = \frac{\sum_j w_{ij}^z}{\sum_{ij} w_{ij}^z}, \text{ for } z = s, t. \quad (4)$$

The GW distance between \mathcal{G}^s and \mathcal{G}^t is then defined as

$$\begin{aligned} GW(\boldsymbol{\mu}^s, \boldsymbol{\mu}^t) &= \min_{\mathbf{T} \in \Pi(\boldsymbol{\mu}^s, \boldsymbol{\mu}^t)} \sum_{i,j,i',j'} \ell(c_{ij}^s, c_{i'j'}^t) T_{ii'} T_{jj'} \\ &= \min_{\mathbf{T} \in \Pi(\boldsymbol{\mu}^s, \boldsymbol{\mu}^t)} \langle \mathbf{L}(\mathbf{C}^s, \mathbf{C}^t, \mathbf{T}), \mathbf{T} \rangle, \end{aligned} \quad (5)$$

where $\ell(c_{ij}^s, c_{i'j'}^t)$ measures the distance between two scalars c_{ij}^s and $c_{i'j'}^t$. Accordingly, $\mathbf{L}(\mathbf{C}^s, \mathbf{C}^t, \mathbf{T}) = [l_{jj'}] \in \mathbb{R}^{|\mathcal{V}^s| \times |\mathcal{V}^t|}$ and each $l_{jj'} = \sum_{i,i'} \ell(c_{ij}^s, c_{i'j'}^t) T_{ii'}$. The optimal transport map indicates the correspondence of vertices across the two graphs.

2.4 Heterogeneous Graphs

A heterogeneous graph contains multiple types of nodes and edges. Random walk based methods are often employed to capture the structural properties of heterogeneous graphs Cai et al. [2018]; Zhang et al. [2019]; Shi et al. [2019]. To form a random walk path, they recursively select one adjacent vertex of the current vertex at random. When the number of vertices within the path reaches a pre-set number called *walk length* η , the sampling procedure terminates. After repeating the above procedure ι times to gather random walk paths, one can capture the *proximities* among vertices carried by the graph and construct the neighbourhood \mathcal{N}_u of vertex u . Neural networks like LSTM are then applied to generate node embeddings which preserve the vertex *proximities* Cai et al. [2018]; Zhang et al. [2019]. Specifically, one can learn the embedding vector of each node by optimizing the following objective

$$\max_f \sum_{u \in \mathcal{V}} \log \mathbb{P}(\mathcal{N}_u | f(u)),$$

where $\mathbb{P}(\cdot)$ denotes the probability an event happens, $f : \mathcal{V} \rightarrow \mathbb{R}^d$ is the neural network to be trained.

3 Partial OT for Graph Matching

Our method unifies partial optimal transport-based graph matching and node embedding in the same framework and allows them to benefit each other. In this section, we describe critical details of PPGM and summarize it in Algorithm 1.

²In this paper, we use words "vertex" and "node" interchangeably.

3.1 Proposed Model

We simultaneously learn the transport map \mathbf{T} indicating the correspondence between graphs and the node embeddings \mathbf{Z}^s and \mathbf{Z}^t that are parameterized by θ^s and θ^t respectively, which leads to the following optimization objective

$$\begin{aligned} \min_{\mathbf{T}, \theta^s, \theta^t} & \left\langle \mathbf{L}(\mathbf{C}^s(\theta^s), \mathbf{C}^t(\theta^t), \mathbf{T}), \mathbf{T} \right\rangle \\ & + \alpha \left\langle \mathbf{K}(\mathbf{Z}^s(\theta^s), \mathbf{Z}^t(\theta^t)), \mathbf{T} \right\rangle + \alpha_1 R(\mathbf{Z}^s(\theta^s), \mathbf{Z}^t(\theta^t)), \end{aligned} \quad (6)$$

subject to $\mathbf{T} \in \Pi^b(\boldsymbol{\mu}^s, \boldsymbol{\mu}^t)$, where we explain the three terms as follows

1. The GW-distance $\left\langle \mathbf{L}(\mathbf{C}^s(\theta^s), \mathbf{C}^t(\theta^t), \mathbf{T}), \mathbf{T} \right\rangle$ is the cost for pairwise assignment. $\mathbf{C}^s(\theta^s)$ and $\mathbf{C}^t(\theta^t)$ are defined as follows

$$\mathbf{C}^z(\theta^z) = (1 - \alpha)\mathbf{G}^z + \alpha\mathbf{K}(\mathbf{Z}^z(\theta^z), \mathbf{Z}^z(\theta^z)), \quad (7)$$

for $z = s, t$, where $\mathbf{G}^z = [g(w_{ij}^z)] \in \mathbb{R}^{|\mathcal{V}^z| \times |\mathcal{V}^z|}$ represents the dissimilarity derived according to the graph weight matrix \mathbf{W}^z , $\mathbf{K}(\mathbf{Z}^z(\theta^z), \mathbf{Z}^z(\theta^z)) = [k(\mathbf{z}_i(\theta^z), \mathbf{z}_j(\theta^z))] \in \mathbb{R}^{|\mathcal{V}^z| \times |\mathcal{V}^z|}$ with each element $k(\mathbf{z}_i(\theta^z), \mathbf{z}_j(\theta^z))$ measuring the difference between node embeddings \mathbf{z}_i and \mathbf{z}_j within the same graph. $g(\cdot)$ and $k(\cdot, \cdot)$ can take forms as in Sec. 5. α is a hyperparameter characterizing the contribution of embedding-based dissimilarity to $\mathbf{C}^z(\theta^z)$.

2. The Wasserstein distance $\left\langle \mathbf{K}(\mathbf{Z}^s(\theta^s), \mathbf{Z}^t(\theta^t)), \mathbf{T} \right\rangle = \sum_{i,i'} T_{ii'} k(\mathbf{z}_i(\theta^s), \mathbf{z}_{i'}(\theta^t))$ measures the cost induced by unary assignment. This term is also based on the difference between node embeddings, and its contribution is controlled by the same hyperparameter α , following Xu et al. [2019b].
3. $R(\mathbf{Z}^s(\theta^s), \mathbf{Z}^t(\theta^t))$ regularizes the embedding learning and is formulated in Sec. 3.3 and 4.2 for homogeneous and heterogeneous graphs, respectively.

Although (6) is a complicated non-convex optimization problem, we can solve it effectively by alternately updating the transport map and the embedding, as we shall see in the next two subsections.

3.2 Learning Optimal Transport

Given θ_m^s and θ_m^t , we solve the following sub-problem

$$\min_{\mathbf{T}} \left\langle \mathbf{L}(\mathbf{C}^s(\theta_m^s), \mathbf{C}^t(\theta_m^t), \mathbf{T}) + \alpha\mathbf{K}(\mathbf{Z}^s(\theta_m^s), \mathbf{Z}^t(\theta_m^t)), \mathbf{T} \right\rangle, \quad (8)$$

subject to $\mathbf{T} \in \Pi^b(\boldsymbol{\mu}^s, \boldsymbol{\mu}^t)$. Following Xie et al. [2018]; Xu et al. [2019b], we solve (8) iteratively with a proximal point method. Specifically, in the n -th iteration, we update \mathbf{T} by solving

$$\begin{aligned} \min_{\mathbf{T} \in \Pi^b(\boldsymbol{\mu}^s, \boldsymbol{\mu}^t)} & \left\langle \mathbf{L}(\mathbf{C}^s(\theta_m^s), \mathbf{C}^t(\theta_m^t), \mathbf{T}) \right. \\ & \left. + \alpha\mathbf{K}(\mathbf{Z}^s(\theta_m^s), \mathbf{Z}^t(\theta_m^t)), \mathbf{T} \right\rangle + \gamma KL(\mathbf{T} \| \mathbf{T}_n), \end{aligned} \quad (9)$$

When we use projected gradient descent to solve (9) with the learning rate $\frac{1}{\gamma}$, (9) is equivalent to the following entropy regularized optimal transport problem

$$\begin{aligned} \min_{\mathbf{T} \in \Pi^b(\boldsymbol{\mu}^s, \boldsymbol{\mu}^t)} & \left\langle \mathbf{L}(\mathbf{C}^s(\theta_m^s), \mathbf{C}^t(\theta_m^t), \mathbf{T}_n) - \gamma - \gamma \log \mathbf{T}_n \right. \\ & \left. + \alpha\mathbf{K}(\mathbf{Z}^s(\theta_m^s), \mathbf{Z}^t(\theta_m^t)), \mathbf{T} \right\rangle + \gamma H(\mathbf{T}). \end{aligned} \quad (10)$$

Proposition 1 Let \mathbf{T}^* and $\bar{\mathbf{T}}^*$ be the optimal transport plans of the partial Wasserstein problem and the extended Wasserstein problem respectively, i.e., $\mathbf{T}^* = \arg \min_{\mathbf{T} \in \Pi^b(\mathbf{p}, \mathbf{q})} \langle \mathbf{J}, \mathbf{T} \rangle$ and $\bar{\mathbf{T}}^* = \arg \min_{\bar{\mathbf{T}} \in \Pi(\bar{\mathbf{p}}, \bar{\mathbf{q}})} \langle \bar{\mathbf{J}}, \bar{\mathbf{T}} \rangle$, where the extended cost matrix is defined as $\bar{\mathbf{J}} = \begin{bmatrix} \mathbf{J} & \xi \mathbf{1} \\ \xi \mathbf{1}^\top & +\infty \end{bmatrix}$ with ξ being any bounded scalar, and extended margins are given by $\bar{\mathbf{p}} = [\mathbf{p}, 1 - b]^\top$ and $\bar{\mathbf{q}} = [\mathbf{q}, 1 - b]^\top$. Then one has

$$W_p^p(\bar{\mathbf{p}}, \bar{\mathbf{q}}) - PW_p^p(\mathbf{p}, \mathbf{q}) = \xi(2 - 2b),$$

and \mathbf{T}^* equals $\bar{\mathbf{T}}^*$ deprived from its last row and last column.

The proof is deferred to the Appendix.

Remark. Extending the cost matrix is equivalent to adding a *dummy* point to \mathcal{G}^s and \mathcal{G}^t respectively in our partial graph matching problem. Nodes that are not matched to the two dummy nodes are considered to have counterparts in the other graph. When $b = 1$, the partial graph matching problem is reduced to full graph matching. We can control the number of matched node pairs by varying b , as is depicted in Figure 1.

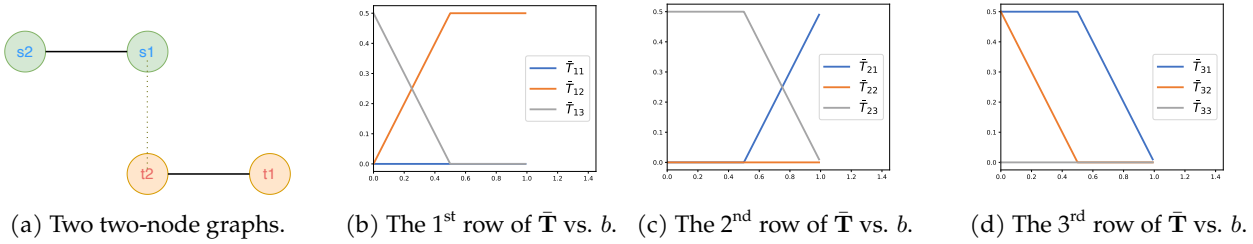


Figure 1: Matching result of a pair of two-node graphs for varying b when we only consider the Wasserstein distance with cost matrix $\mathbf{K}(\mathbf{Z}^s(\theta^s), \mathbf{Z}^t(\theta^t)) = \begin{bmatrix} 2 & -1 \\ 1 & 2 \end{bmatrix}$. The dotted line denotes the ground truth correspondence, i.e., only node s_1 in the source graph has its counterpart. By definition, $\mu^s = \mu^t = [0.5, 0.5]^\top$. For each node in the source graph, we select its matched node according to the calculated extended transport plan $\bar{\mathbf{T}}$, which we demonstrate in Figure 1b and Figure 1c. If $0.75 < b \leq 1$, s_1 is matched to t_2 and s_2 is matched to t_1 . If $0.25 < b < 0.75$, only s_1 is matched to t_2 while s_2 is matched to the dummy node in the target graph. If $0 < b < 0.25$, both s_1 and s_2 are matched to the dummy node. Therefore, we can correctly recover the correspondence of nodes with $0.25 < b < 0.75$.

Proposition 1 implies that Eq. (10) can be solved using Sinkhorn-Knopp algorithm with linear convergence Sinkhorn and Knopp [1967]; Cuturi [2013]. Hence, we decompose (8) into a sequence of sub-problems, each of which is then solved via the projected gradient descent. The convergence is guaranteed as follows.

Proposition 2 Every limit point generated by the above procedure, i.e., $\lim_{n \rightarrow \infty} \mathbf{T}_n$, is a stationary point of Eq. (8).

The proof is given in the appendix.

Complexity for learning optimal transport. One of the most computationally expensive steps in calculating the optimal transport given stored embeddings, is evaluating $\mathbf{L}(\mathbf{C}^s(\theta_m^s), \mathbf{C}^t(\theta_m^t), \mathbf{T}_n)$. Fortunately, $\mathbf{L}(\mathbf{C}^s(\theta_m^s), \mathbf{C}^t(\theta_m^t), \mathbf{T}_n)$ can be computed efficiently when common loss functions like square loss or KL divergence are adopted for $\ell(\cdot, \cdot)$ Peyré et al. [2016]; Xu et al. [2019b]. To be more specific, $\ell(a, b)$ can be written as $\ell(a, b) = d_1(a) + d_2(b) - h_1(a)h_2(b)$. Then the loss matrix \mathbf{L} can be obtained by performing element-wise operations as $\mathbf{L}(\mathbf{C}^s(\theta_m^s), \mathbf{C}^t(\theta_m^t), \mathbf{T}_n) = d_1(\mathbf{C}^s(\theta_m^s)) \mu^s \mathbf{1}_{|\mathcal{V}^t|}^\top + \mathbf{1}_{|\mathcal{V}^s|} \mu^{t^\top} d_2(\mathbf{C}^t(\theta_m^t)) - h_1(\mathbf{C}^s(\theta_m^s)) \mathbf{T}_n h_2(\mathbf{C}^t(\theta_m^t))$. Because \mathbf{T} tends to be sparse quickly Peyré et al. [2016]; Xu et al. [2019b], $\mathbf{L}(\mathbf{C}^s, \mathbf{C}^t, \mathbf{T})$ involves computational complexity $\mathcal{O}(V^3)$, where $V = \max\{|\mathcal{V}^s|, |\mathcal{V}^t|\}$. Given the embedding vectors, the computational cost

for $\mathbf{K}(\mathbf{Z}^s(\boldsymbol{\theta}^s), \mathbf{Z}^t(\boldsymbol{\theta}^t))$ is $\mathcal{O}(V^2d)$, where d is the dimension of embeddings. In addition, if we run Sinkhorn-Knopp algorithm for N iterations, the complexity is $\mathcal{O}(NV^3)$. Therefore, $\mathcal{O}(V^2d + NV^3)$ computational cost is involved in learning the optimal transport.

3.3 Updating Embeddings

With slight abuse of notation, let $\ell(\cdot, \cdot)$ in Eq. (5) be an element-wise loss function. Then $R(\mathbf{Z}^s(\boldsymbol{\theta}^s), \mathbf{Z}^t(\boldsymbol{\theta}^t))$ for homogeneous graphs is given by

$$\sum_{z=s,t} \ell\left(\mathbf{K}(\mathbf{Z}^z(\boldsymbol{\theta}^z), \mathbf{Z}^z(\boldsymbol{\theta}^z)), \mathbf{G}^k\right) + \underbrace{\ell\left(\mathbf{K}(\mathbf{Z}^s(\boldsymbol{\theta}^s), \mathbf{Z}^t(\boldsymbol{\theta}^t)), \mathbf{G}^{st}\right)}_{\text{optional}}. \quad (11)$$

Note that if some ground truth correspondences across \mathcal{G}^s and \mathcal{G}^t are available, we can calculate a distance matrix between the two graphs, denoted as $\mathbf{G}^{st} \in \mathbb{R}^{|\mathcal{V}^s| \times |\mathcal{V}^t|}$, and require the distance between the embeddings to be close to \mathbf{G}^{st} , as shown in Eq. (11).

Given the learned transport plan $\hat{\mathbf{T}}_m$, we update the embeddings as follows

$$\begin{aligned} & \min_{\boldsymbol{\theta}^s, \boldsymbol{\theta}^t} \left\langle \mathbf{L}(\mathbf{C}^s(\boldsymbol{\theta}^s), \mathbf{C}^t(\boldsymbol{\theta}^t), \hat{\mathbf{T}}_m), \hat{\mathbf{T}}_m \right\rangle \\ & + \alpha \left\langle \mathbf{K}(\mathbf{Z}^s(\boldsymbol{\theta}^s), \mathbf{Z}^t(\boldsymbol{\theta}^t)), \hat{\mathbf{T}}_m \right\rangle + \alpha_1 R(\mathbf{Z}^s(\boldsymbol{\theta}^s), \mathbf{Z}^t(\boldsymbol{\theta}^t)), \end{aligned} \quad (12)$$

which can be solved effectively by SGD. Note that $\boldsymbol{\theta}^s$ and $\boldsymbol{\theta}^t$ are initialized randomly and \mathbf{Z}^s and \mathbf{Z}^t are thus unreliable at early iterations. We adjust α as follows: with the total number of rounds as M , in the m -th iteration, we set $\alpha = \frac{m}{M}$. PPGM is summarized in Algorithm 1. Both the vertex embedding and the optimal transport learning can be conducted on GPUs.

Algorithm 1 Partial optimal transport-based Partial Graph Matching (PPGM)

- 1: **Input:** α_1 , total rounds M , graphs \mathcal{G}^s and \mathcal{G}^t , total transport mass b .
 - 2: **Output:** Correspondence set \mathcal{C} .
 - 3: Initialize $\boldsymbol{\theta}^s$ and $\boldsymbol{\theta}^t$ randomly, $\hat{\mathbf{T}}_0 = \boldsymbol{\mu}^s \boldsymbol{\mu}^{t\top}$.
 - 4: **for** $m = 0, \dots, M - 1$ **do**
 - 5: $\alpha = \frac{m}{M}$
 - 6: Calculate $\hat{\mathbf{T}}_{m+1}$ by solving (8).
 - 7: Update embedding via solving (12) or (13)
 - 8: Store the embedding
 - 9: **end for**
 - 10: $\hat{\mathbf{T}} = \hat{\mathbf{T}}_M$
 - 11: $\tilde{\mathbf{T}} = [\hat{\mathbf{T}}, \mathbf{1} - \hat{\mathbf{T}}\mathbf{1}]$
 - 12: Initialize correspondence set $\mathcal{C} = \emptyset$
 - 13: **for** $u_i \in \mathcal{V}^s$ **do**
 - 14: $j = \arg \max_j \tilde{T}_{ij}$.
 - 15: **if** $j \neq (|\mathcal{V}^t| + 1)$ **then**
 - 16: $\mathcal{C} = \mathcal{C} \cup \{(u_i, v_j)\}$
 - 17: **end if**
 - 18: **end for**
-

4 Heterogeneous Graph Matching

In this section, we apply PPGM to heterogeneous graph matching. The main step-up lies in an embedding learning method.

4.1 Heterogeneous Network Embedding

In this subsection, we elaborate how we obtain the embeddings $\{f(u; \theta^z) | u \in \mathcal{V}^z, z = s, t\}$, which consists of three parts: (1) sampling heterogeneous neighbours; (2) encoding contents; (3) aggregating heterogeneous neighbours.

Sampling heterogeneous neighbours. We adopt a random walk with restart strategy $\text{RWR}(p, \eta, \iota, n)$ to determine the set of neighbours $\{\mathcal{N}_u^z | u \in \mathcal{V}^z, z = s, t\}$ Tong et al. [2006]; Zhang et al. [2019]. It contains two steps:

1. For each graph \mathcal{G}^z , $z = s, t$, we start a random walk from vertex $u \in \mathcal{V}^z$ and iteratively travels to a randomly selected adjacent vertex. With probability p , the walk returns to the starting vertex.
2. After sampling ι random walk paths (each has length η), for each vertex type r , we choose the n most frequent vertices as the r -type neighbours of u , denoted as $\mathcal{N}_{r,u}^z$. Different types of neighbours are then grouped together to form \mathcal{N}_u^z , i.e., $\mathcal{N}_u^z = \cup_r \mathcal{N}_{r,u}^z$.

Such procedure makes use of the local topological structure of the graph and is more flexible than meta-path based approaches Sun et al. [2011]; Shi et al. [2019].

Encoding contents. We use a multilayer perceptron $\text{MLP-}r$ to encode contents for the r -type vertices. Specifically, we denote the feature representation of vertex $u \in \mathcal{V}^z$ as $\mathbf{x}_u \in \mathbb{R}^D$. The content is then encoded using $\text{MLP} : \mathbb{R}^D \rightarrow \mathbb{R}^d$ where d is the dimension of an embedding vector, i.e.,

$$f_1(u) = \text{MLP}(\mathbf{x}_u; \theta_{\text{MLP-}r}^z),$$

for vertex u of type r and $z = s, t$.

ρ	0.7			0.5			0.3		
	recall	precision	F1	recall	precision	F1	recall	precision	F1
SuperGlue	.40 ± .10	.36 ± .12	.38 ± .11	.40 ± .10	.33 ± .08	.36 ± .09	.23 ± .01	.19 ± .01	.21 ± .01
ZAC	.69 ± .03	.62 ± .01	.65 ± .02	.35 ± .07	.30 ± .08	.32 ± .07	.20 ± .02	.17 ± .02	.19 ± .02
BB-GM	.25 ± .03	.20 ± .03	.23 ± .03	.22 ± .04	.16 ± .03	.18 ± .03	.19 ± .03	.12 ± .01	.14 ± .01
PPGM	.83 ± .02	.73 ± .01	.78 ± .02	.46 ± .02	.42 ± .01	.44 ± .01	.38 ± .02	.35 ± .03	.36 ± .02

Table 1: The performance of PPGM and state-of-the-art methods on K-NN graph datasets with varying overlap ratio ρ .

Aggregating Neighbours. Aggregating content vectors $\{f_1(u) | u \in \mathcal{V}^z, z = s, t\}$ includes two steps:

1. *Same type neighbours aggregation.* We employ Bi-LSTM networks to aggregate content vectors for $\mathcal{N}_{r,u}^k$, i.e.,

$$f_2^r(u) = \frac{1}{|\mathcal{N}_{r,u}^z|} \sum_{u' \in \mathcal{N}_{r,u}^z} \left[\vec{\text{LSTM}}(f_1(u'); \theta_{\text{LSTM-}r}^z) \oplus \overleftarrow{\text{LSTM}}(f_1(u'); \theta_{\text{LSTM-}r}^z) \right],$$

for vertices u' of type r , where $\text{LSTM} : \mathbb{R}^d \rightarrow \mathbb{R}^{d/2}$ and \oplus means vector concatenation.

2. *Types combination.* Different types of neighbours make different contributions to the final embeddings. To combine the vectors generated by the previous step, we adopt an attention mechanism Veličković et al. [2017]. The output embedding vector is thus defined as

$$f(u) = \sum_{f_i \in \mathcal{F}(u)} a^{u,i} f_i, \text{ with}$$

$$a^{u,i} = \frac{\exp(\text{LeakyReLU}(\mathbf{h}_u^\top [f_i \oplus f_1(u)]))}{\sum_{f_i \in \mathcal{F}(u)} \exp(\text{LeakyReLU}(\mathbf{h}_u^\top [f_i \oplus f_1(u)]))}$$

where $\mathcal{F}(u) = \{f_1(u) \cup (f_2^r(u), \forall r)\}$, attention parameter $a^{u,i}$ indicates the importance of component vectors and \mathbf{h}_u is the parameter to be learned.

Leveraging the *negative sampling* technique Mikolov et al. [2013]; Cai et al. [2018]; Zhang et al. [2019], $\log \mathbb{P}(\mathcal{N}_u^z | f(u; \boldsymbol{\theta}^z))$ in Sec. 2.4 is defined as follows

$$\log \mathbb{P}(\mathcal{N}_u^z | f(u; \boldsymbol{\theta}^z)) = \sum_{u_p \in \mathcal{N}_{r,u}^z} \log \sigma(f(u; \boldsymbol{\theta}^z)^\top f(u_p; \boldsymbol{\theta}^z))$$

$$+ \sum_{u_n \in \mathcal{V}^z \setminus \mathcal{N}_u^z} \log \sigma(-f(u; \boldsymbol{\theta}^z)^\top f(u_n; \boldsymbol{\theta}^z)),$$

where $z = s, t, r$ is the type of u , $\sigma(\cdot)$ is the sigmoid function, and $\boldsymbol{\theta}^z = [\boldsymbol{\theta}_{\text{MLP-}r}^z \oplus \boldsymbol{\theta}_{\text{LSTM-}r}^z | \forall r] \oplus [\mathbf{h}_u | u \in \mathcal{N}^z]$.

ρ	0.7			0.5			0.3		
	recall	precision	F1	recall	precision	F1	recall	precision	F1
SuperGlue	.34 ± .06	.31 ± .05	.32 ± .05	.29 ± .03	.25 ± .04	.27 ± .04	.26 ± .02	.19 ± .01	.22 ± .01
ZAC	.37 ± .03	.34 ± .04	.35 ± .04	.34 ± .01	.30 ± .01	.32 ± .01	.24 ± .06	.21 ± .06	.23 ± .06
BB-GM	.31 ± .07	.26 ± .06	.28 ± .06	.25 ± .03	.19 ± .02	.21 ± .03	.18 ± .01	.12 ± .01	.14 ± .01
PPGM	.64 ± .09	.54 ± .08	.58 ± .08	.55 ± .06	.43 ± .06	.48 ± .06	.48 ± .06	.35 ± .05	.40 ± .05

Table 2: The performance of PPGM and state-of-the-art methods on BA graph datasets with varying overlap ratio ρ .

4.2 Increasing Inter-type Separability

We explicitly use the type information to increase the separability of inter-type embedding vectors. Let \mathcal{H}^K be the Reproducing Kernel Hilbert Space induced by feature map $f(\cdot)$, with K being the kernel. Then the optimal classifier for different types of nodes takes the form $h(\mathbf{z}) = \sum_{i=1}^n \beta_i K(\mathbf{z}_i, \mathbf{z})$ by the Representer Theorem Belkin et al. [2006], where $\boldsymbol{\beta} = [\beta_1, \dots, \beta_n]^\top$ is the coefficients vector. To sum it up, $R(\mathbf{Z}^s(\boldsymbol{\theta}^s), \mathbf{Z}^t(\boldsymbol{\theta}^t))$ for heterogeneous graph matching is defined as

$$R(\mathbf{Z}^s(\boldsymbol{\theta}^s), \mathbf{Z}^t(\boldsymbol{\theta}^t)) = \sum_{z=s,t} \left(-\log \mathbb{P}(\mathcal{N}_u^z | f(u; \boldsymbol{\theta}^z)) \right.$$

$$\left. + \zeta \sum_{u \in \mathcal{V}^z} (r_u - h^z(\mathbf{z}(\boldsymbol{\theta}^z)))^2 \right).$$

Therefore, given the optimal transport $\hat{\mathbf{T}}_m$ obtained in (8), we update the embeddings by solving the following optimization problem

$$\begin{aligned}
& \min_{\boldsymbol{\theta}^s, \boldsymbol{\theta}^t, \boldsymbol{\beta}^s, \boldsymbol{\beta}^t} \left(\mathbf{L}(\mathbf{C}^s(\boldsymbol{\theta}^s), \mathbf{C}^t(\boldsymbol{\theta}^t), \hat{\mathbf{T}}_m), \hat{\mathbf{T}}_m) \right. \\
& \quad \left. + \alpha \left(\mathbf{K}(\mathbf{Z}^s(\boldsymbol{\theta}^s), \mathbf{Z}^t(\boldsymbol{\theta}^t)), \hat{\mathbf{T}}_m \right) \right. \\
& \quad \left. + \alpha_1 \sum_{z=s,t} \left(-\log \mathbb{P}(\mathcal{N}_u^z | f(u; \boldsymbol{\theta}^z)) \right) \right. \\
& \quad \left. + \zeta \sum_{u \in \mathcal{V}^z} \left(r_u - h^z(\mathbf{z}(\boldsymbol{\theta}^z)) \right)^2 \right), \tag{13}
\end{aligned}$$

where r_u is the type of u and the last line is the proposed regularizer promoting the separability of inter-type embeddings.

Our method learns node embeddings of the two graphs on the same manifold. By explicitly using the type information of vertices, we distribute embeddings of different types of vertices to different regions of the manifold. As is shown in Figure 2, the distances between embedding vectors indicate the correspondence across the two graphs.

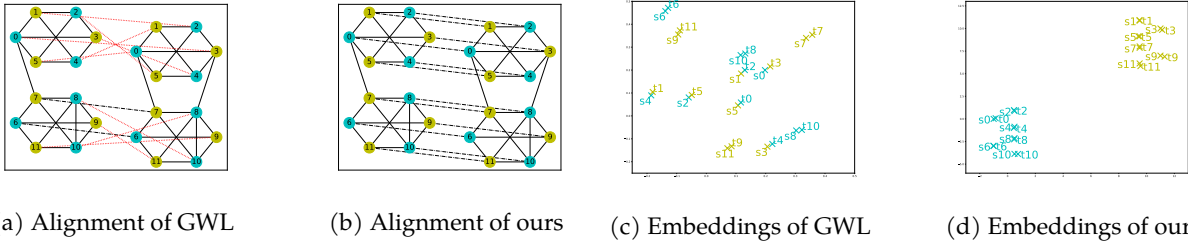


Figure 2: Comparison of node alignments and embedding vectors between our method (with $b = 1$) and GWL Xu et al. [2019b], a Gromov-Wasserstein learning algorithm that disregards the type information of nodes, on a toy example. We denote correct and wrong alignments by black dashed lines and red dotted lines, respectively. Our method successfully aligns all nodes while GWL only aligns two pairs of nodes correctly. Figure 2c and Figure 2d demonstrate that the distances between embedding vectors directly indicate the node correspondence. In GWL, embedding vectors of different types are in the same region and cannot be distinguished, which worsens the alignment.

Note that while the last term in Eq. (13) increases the separability of inter-class embeddings, it may reduce the distances between intra-class embedding vectors. Therefore ζ is usually a small number and the last term only regularizes the node embedding for heterogenous graphs. Problem (13) can also be solved efficiently by SGD.

5 Experiments

We apply the proposed framework to both synthetic graphs and real-world graphs, and compare it with state-of-the-art partial matching methods, including SuperGlue Sarlin et al. [2020], ZAC Wang et al. [2020a], and BB-GMRolínek et al. [2020]. In our experiments, we set $\ell(\cdot, \cdot)$ as the square loss, $g(w_{ij}) = \frac{1}{1+w_{ij}}$, and $k(\mathbf{z}_i, \mathbf{z}_j) = 1 - \exp\left(-\delta\left(1 - \frac{\mathbf{z}_i^\top \mathbf{z}_j}{\|\mathbf{z}_i\| \|\mathbf{z}_j\|}\right)\right)$. Adam is chosen as the optimizer for Eq. (12) and (13). For better evaluation of partial graph matching, we compute the commonly used indicators called recall, precision,

and F-measure,

$$\begin{aligned} \text{recall} &= \frac{\#\{\text{correct matching}\}}{\#\{\text{ground truth matching}\}}, \\ \text{precision} &= \frac{\#\{\text{correct matching}\}}{\#\{\text{total predicted matching}\}}, \\ \text{F1} &= 2 \frac{\text{recall} \cdot \text{precision}}{\text{recall} + \text{precision}}. \end{aligned}$$

We fine-tune all methods to obtain the best performance. Each tested method is run for 5 times. The source code is included in the supplementary.

5.1 Homogeneous Synthetic Datasets

We first verify the efficacy of our framework on two kinds of commonly used synthetic datasets, K-NN graph datasets [Wikipedia contributors \[2020\]](#) and BA graph datasets [Barabási et al. \[2016\]](#). For both kinds of graphs, we sample the feature content vectors from Gaussian distributions $N(\mathbf{0}, \mathbf{1})$ and we slightly disturb the feature vectors in the target graph, that is, if $u_i \in \mathcal{V}^s$ and $u_{i'} \in \mathcal{V}^t$ are counterparts, the feature vector of $u_{i'}$ is given by $\mathbf{x}_{i'}^t = \mathbf{x}_i^s + 0.1\sigma_{i'}$, where $\sigma_{i'} \sim N(\mathbf{0}, \mathbf{1})$. For the K-NN graphs, an edge connects vertex u and v if the distance between u and v is among the k smallest distances from u to other nodes in the graph. We add new nodes and edges to the BA graphs following the *growth* procedure of the BA model, i.e., each new node is connected to m existing nodes with a probability that is proportional to the number of links that the existing nodes already have. We set the weight of each edge connecting two nodes in one graph as the cosine similarity, i.e., $w_{ij}^z = \frac{1}{2} + \frac{(\mathbf{x}_i^z, \mathbf{x}_j^z)}{2\|\mathbf{x}_i^z\|\|\mathbf{x}_j^z\|}$ for $z = s, t$. The datasets have $k = 3$, $m = 3$, and $\#\{\text{ground truth matching}\} = 50$ when we generate the graphs. We report the performance of PPGM for varying overlap ratios in [Table 1](#) and [Table 2](#). Formally, the overlap ratio is defined as $\rho = \frac{\#\{\text{ground truth matching}\}}{\min\{|\mathcal{V}^s|, |\mathcal{V}^t|\}}$. We set $\alpha_1 = 1 \times 10^{-2}$ and the total transport mass $b = \rho$. As is shown, PPGM consistently outperforms state-of-the-art methods on both types of graphs. With the overlap ratio decreasing, the performance of all methods deteriorates. Such phenomenon is also observed in [Wang et al. \[2020a\]](#).

5.2 Heterogeneous Real-world Graphs

Data	Node	Edge
Source Graph	# author: 286	# author-paper: 618
	# paper: 286	# paper-paper: 133
	# venue: 18	# paper-venue: 286
Target Graph	# author: 286	# author-paper: 618
	# paper: 286	# paper-paper: 123
	# venue: 18	# paper-venue: 286

Table 3: Datasets used in the heterogeneous graph matching experiment.

We extract two academic social networks from the public Aminer data³ and preprocess data following [Zhang et al. \[2019\]](#). The main statistics of the graphs are summarized in [Table 3](#). The overlap ratio for the three types of nodes {author, paper, venue} is 0.7, 0.7, and 1 respectively. We set $\alpha_1 = 1 \times 10^{-2}$, $\zeta = 1 \times 10^{-4}$ and $b = 0.7$. PPGM excels all baseline methods by 77% in terms of F-measure.

Due to the limited space, more experimental results are provided in the supplementary material.

³<https://www.aminer.org/data>

method	recall	precision	F1
SuperGlue	.019 ± .005	.026 ± .008	.022 ± .006
ZAC	.006 ± .001	.005 ± .001	.005 ± .001
BB-GM	.001 ± .001	.005 ± .005	.002 ± .002
PPGM	.030 ± .007	.058 ± .011	.039 ± .006

Table 4: The performance of PPGM and state-of-the-art methods on academic social networks.

6 Conclusion

In this paper, we propose a novel partial Gromov-Wasserstein learning framework for partially matching both homogeneous graphs and heterogeneous graphs. Our framework models the source graph and the target graph as discrete distributions and transports a fraction of the probability mass to match nodes that are relatively similar. Incorporating the heterogeneous embedding learning, our framework can match general heterogeneous graphs. Empirical results demonstrate that our framework can improve the graph alignment quality. In the future, we plan to extend our framework to multi-graph matching, graph partitioning, graph compression, and network retrieval.

Ethics Statement

This work proposes a framework for partially matching graphs, which has many applications including aligning protein-protein networks from different species, linking user accounts in social platforms, aligning entities in knowledge graphs, to name a few. Our framework can improve the matching quality hence benefit these applications. We admit that negative aspects may exist. Our framework basically does not raise ethical concerns. But when it is maliciously used, our framework can be used to determine the identity of anonymous users in a social platform and cause privacy leakage problems.

References

- Albert-László Barabási et al. *Network science*. Cambridge university press, 2016.
- Amélie Barbe, Marc Sebban, Paulo Gonçalves, Pierre Borgnat, and Rémi Gribonval. Graph diffusion wasserstein distances. In *European Conference on Machine Learning and Principles and Practice of Knowledge Discovery in Databases*, 2020.
- Mikhail Belkin, Partha Niyogi, and Vikas Sindhwani. Manifold regularization: A geometric framework for learning from labeled and unlabeled examples. *Journal of machine learning research*, 7(Nov):2399–2434, 2006.
- Stefano Berretti, Alberto Del Bimbo, and Enrico Vicario. Efficient matching and indexing of graph models in content-based retrieval. *IEEE Transactions on Pattern Analysis and Machine Intelligence*, 23(10):1089–1105, 2001.
- Tibério S Caetano, Julian J McAuley, Li Cheng, Quoc V Le, and Alex J Smola. Learning graph matching. *IEEE transactions on pattern analysis and machine intelligence*, 31(6):1048–1058, 2009.
- Luis A Caffarelli and Robert J McCann. Free boundaries in optimal transport and monge-ampere obstacle problems. *Annals of mathematics*, pages 673–730, 2010.
- Hongyun Cai, Vincent W Zheng, and Kevin Chen-Chuan Chang. A comprehensive survey of graph embedding: Problems, techniques, and applications. *IEEE Transactions on Knowledge and Data Engineering*, 30(9):1616–1637, 2018.

- Samir Chowdhury and Facundo Mémoli. The gromov–wasserstein distance between networks and stable network invariants. *Information and Inference: A Journal of the IMA*, 8(4):757–787, 2019.
- Marco Cuturi. Sinkhorn distances: Lightspeed computation of optimal transport. In *NeurIPS*, pages 2292–2300, 2013.
- Jie Feng, Mingyang Zhang, Huandong Wang, Zeyu Yang, Chao Zhang, Yong Li, and Depeng Jin. Dplink: User identity linkage via deep neural network from heterogeneous mobility data. In *The World Wide Web Conference*, pages 459–469, 2019.
- Alessio Figalli. The optimal partial transport problem. *Archive for rational mechanics and analysis*, 195(2): 533–560, 2010.
- Shawn Gu, John Johnson, Fazle E Faisal, and Tijana Milenković. From homogeneous to heterogeneous network alignment via colored graphlets. *Scientific reports*, 8(1):1–16, 2018.
- Ehsan Kazemi, Lyudmila Yartseva, and Matthias Grossglauser. When can two unlabeled networks be aligned under partial overlap? In *2015 53rd Annual Allerton Conference on Communication, Control, and Computing (Allerton)*, pages 33–42. IEEE, 2015.
- Nil Mamano and Wayne B Hayes. Sana: simulated annealing far outperforms many other search algorithms for biological network alignment. *Bioinformatics*, 33(14):2156–2164, 2017.
- Hermina Petric Maretic, Mireille El Gheche, Giovanni Chierchia, and Pascal Frossard. Got: an optimal transport framework for graph comparison. In *NeurIPS*, pages 13876–13887, 2019.
- Hermina Petric Maretic, Mireille El Gheche, Matthias Minder, Giovanni Chierchia, and Pascal Frossard. Wasserstein-based graph alignment. *arXiv preprint arXiv:2003.06048*, 2020.
- Facundo Mémoli. Gromov–wasserstein distances and the metric approach to object matching. *Foundations of computational mathematics*, 11(4):417–487, 2011.
- Tomas Mikolov, Ilya Sutskever, Kai Chen, Greg S Corrado, and Jeff Dean. Distributed representations of words and phrases and their compositionality. In *NeurIPS*, pages 3111–3119, 2013.
- I Burak Özer, Wayne Wolf, and Ali N Akansu. A graph-based object description for information retrieval in digital image and video libraries. *Journal of Visual Communication and Image Representation*, 13(4):425–459, 2002.
- Younghee Park, Douglas Reeves, Vikram Mulukutla, and Balaji Sundaravel. Fast malware classification by automated behavioral graph matching. In *Proceedings of the Sixth Annual Workshop on Cyber Security and Information Intelligence Research*, pages 1–4, 2010.
- Evan Patterson. Hausdorff and wasserstein metrics on graphs and other structured data. *arXiv: Optimization and Control*, 2019.
- Shichao Pei, Lu Yu, Guoxian Yu, and Xiangliang Zhang. Rea: Robust cross-lingual entity alignment between knowledge graphs. In *Proceedings of the 26th ACM SIGKDD International Conference on Knowledge Discovery & Data Mining*, pages 2175–2184, 2020.
- Gabriel Peyré, Marco Cuturi, and Justin Solomon. Gromov-wasserstein averaging of kernel and distance matrices. In *ICML*, pages 2664–2672, 2016.
- Michal Rolínek, Paul Swoboda, Dominik Zietlow, Anselm Paulus, Vít Musil, and Georg Martius. Deep graph matching via blackbox differentiation of combinatorial solvers. *arXiv preprint arXiv:2003.11657*, 2020.
- Paul-Edouard Sarlin, Daniel DeTone, Tomasz Malisiewicz, and Andrew Rabinovich. Superglue: Learning feature matching with graph neural networks. In *CVPR*, pages 4938–4947, 2020.

- Adam Schenker, Mark Last, Horst Bunke, and Abraham Kandel. Classification of web documents using graph matching. *International Journal of Pattern Recognition and Artificial Intelligence*, 18(03):475–496, 2004.
- Chuan Shi, Binbin Hu, Wayne Xin Zhao, and Philip S Yu. Heterogeneous information network embedding for recommendation. *IEEE Transactions on Knowledge and Data Engineering*, 31(2):357–370, 2019.
- Richard Sinkhorn and Paul Knopp. Concerning nonnegative matrices and doubly stochastic matrices. *Pacific Journal of Mathematics*, 21(2):343–348, 1967.
- Yihan Sun, Joseph Crawford, Jie Tang, and Tijana Milenković. Simultaneous optimization of both node and edge conservation in network alignment via wave. In *International Workshop on Algorithms in Bioinformatics*, pages 16–39. Springer, 2015.
- Yizhou Sun, Jiawei Han, Xifeng Yan, Philip S Yu, and Tianyi Wu. Pathsim: Meta path-based top-k similarity search in heterogeneous information networks. *Proceedings of the VLDB Endowment*, 4(11):992–1003, 2011.
- Zequn Sun, Chengming Wang, Wei Hu, Muhao Chen, Jian Dai, Wei Zhang, and Yuzhong Qu. Knowledge graph alignment network with gated multi-hop neighborhood aggregation. In *AAAI*, volume 34, pages 222–229, 2020.
- Paul Swoboda, Ashkan Mokarian, Christian Theobalt, Florian Bernard, et al. A convex relaxation for multi-graph matching. In *CVPR*, pages 11156–11165, 2019.
- Vayer Titouan, Nicolas Courty, Romain Tavenard, and Rémi Flamary. Optimal transport for structured data with application on graphs. In *ICML*, pages 6275–6284, 2019.
- Hanghang Tong, Christos Faloutsos, and Jia-Yu Pan. Fast random walk with restart and its applications. In *ICDM*, pages 613–622. IEEE, 2006.
- Lorenzo Torresani, Vladimir Kolmogorov, and Carsten Rother. A dual decomposition approach to feature correspondence. *IEEE transactions on pattern analysis and machine intelligence*, 35(2):259–271, 2012.
- Petar Veličković, Guillem Cucurull, Arantxa Casanova, Adriana Romero, Pietro Lio, and Yoshua Bengio. Graph attention networks. *arXiv preprint arXiv:1710.10903*, 2017.
- Vipin Vijayan, Vikram Saraph, and Tijana Milenković. Magna++: Maximizing accuracy in global network alignment via both node and edge conservation. *Bioinformatics*, 31(14):2409–2411, 2015.
- Fu-Dong Wang, Nan Xue, Yipeng Zhang, Gui-Song Xia, and Marcello Pelillo. A functional representation for graph matching. *IEEE Transactions on Pattern Analysis and Machine Intelligence*, 2019a.
- Fudong Wang, Nan Xue, Jin-Gang Yu, and Gui-Song Xia. Zero-assignment constraint for graph matching with outliers. In *CVPR*, pages 3033–3042, 2020a.
- Runzhong Wang, Junchi Yan, and Xiaokang Yang. Learning combinatorial embedding networks for deep graph matching. In *ICCV*, pages 3056–3065, 2019b.
- Shen Wang, Zhengzhang Chen, Xiao Yu, Ding Li, Jingchao Ni, Lu-An Tang, Jiaping Gui, Zhichun Li, Haifeng Chen, and Philip S Yu. Heterogeneous graph matching networks for unknown malware detection. In *IJCAI*, pages 3762–3770. AAAI Press, 2019c.
- Tao Wang, He Liu, Yidong Li, Yi Jin, Xiaohui Hou, and Haibin Ling. Learning combinatorial solver for graph matching. In *CVPR*, pages 7568–7577, 2020b.
- Yaqing Wang, Chunyan Feng, Ling Chen, Hongzhi Yin, Caili Guo, and Yunfei Chu. User identity linkage across social networks via linked heterogeneous network embedding. *World Wide Web*, 22(6):2611–2632, 2019d.

- Wikipedia contributors. Nearest neighbor graph — Wikipedia, the free encyclopedia. https://en.wikipedia.org/w/index.php?title=Nearest_neighbor_graph&oldid=956578789, 2020. [Online; accessed 2-June-2020].
- Yujia Xie, Xiangfeng Wang, Ruijia Wang, and Hongyuan Zha. A fast proximal point method for wasserstein distance. *arXiv: Machine Learning*, 2018.
- Hongteng Xu, Dixin Luo, and Lawrence Carin. Scalable gromov-wasserstein learning for graph partitioning and matching. In *NeurIPS*, pages 3046–3056, 2019a.
- Hongteng Xu, Dixin Luo, Hongyuan Zha, and Lawrence Carin. Gromov-wasserstein learning for graph matching and node embedding. *arXiv preprint arXiv:1901.06003*, 2019b.
- Andrei Zanfir and Cristian Sminchisescu. Deep learning of graph matching. In *CVPR*, pages 2684–2693, 2018.
- Chuxu Zhang, Dongjin Song, Chao Huang, Ananthram Swami, and Nitesh V Chawla. Heterogeneous graph neural network. In *Proceedings of the 25th ACM SIGKDD International Conference on Knowledge Discovery & Data Mining*, pages 793–803, 2019.
- Vincent W Zheng, Mo Sha, Yuchen Li, Hongxia Yang, Yuan Fang, Zhenjie Zhang, Kian-Lee Tan, and Kevin Chen-Chuan Chang. Heterogeneous embedding propagation for large-scale e-commerce user alignment. In *ICDM*, pages 1434–1439. IEEE, 2018.
- Xiaochen Zhu, Shaoxu Song, Xiang Lian, Jianmin Wang, and Lei Zou. Matching heterogeneous event data. In *Proceedings of the 2014 ACM SIGMOD International Conference on Management of Data*, pages 1211–1222, 2014.